Available online at www.sciencedirect.com
ScienceDirect
Journal of Nuclear Materials 362 (2007) 438–444
journal of nuclear materials
www.elsevier.com/locate/jnucmat

Ion beam irradiation of lanthanum and thorium-doped yttrium titanates

J. Lian [a], F.X. Zhang [a], M.T. Peters [b], L.M. Wang [c], R.C. Ewing [a,c,*]

[a] Department of Geological Sciences, University of Michigan, Ann Arbor, MI 48109, USA
[b] Argonne National Laboratory, Argonne, IL 60439, USA
[c] Department of Nuclear Engineering and Radiological Sciences, University of Michigan, Ann Arbor, MI 48109, USA

Abstract

$Y_2Ti_2O_7$ pyrochlores doped with La have been sintered at 1373 K for 12 h with the designed compositions of the $(La_xY_{1-x})_2Ti_2O_7$ system ($x = 0$, 0.08, 0.5, and 1), and the phase compositions were analyzed by X-ray diffraction. Limited amounts of La were incorporated into yttrium titanate pyrochlore structure for La-doped samples; while, the end member composition of $La_2Ti_2O_7$ formed a layered perovskite structure. Ion beam-induced amorphization occurred for all compositions in the $(La_xY_{1-x})_2Ti_2O_7$ binary under 1 MeV Kr^{2+} irradiation at room temperature, and the critical amorphization dose decreased with increasing amounts of La^{3+}. The critical amorphization temperatures for $Y_2Ti_2O_7$, $(La_{0.162}Y_{0.838})_2Ti_2O_7$ and $La_2Ti_2O_7$ were determined to be ~780, 890 and 920 K, respectively. Th^{4+} and Fe^{3+}-doped yttrium titanate pyrochlores were synthesized at 1373 K by sintering $Y_2Ti_2O_7$ with $(ThO_2 + Fe_2O_3)$. Pyrochlore structures and the chemical compositions were primarily identified by the X-ray diffraction and energy dispersive X-ray (EDX) measurements. The lattice parameter and the critical amorphization dose (1 MeV Kr^{2+} at room temperature) increase for yttrium titanate pyrochlores with the addition of Th. The increasing 'resistance' to amorphization with less La and greater Th and Fe contents for $(Y_{1-x}La_x)_2Ti_2O_7$ and $Y_2Ti_2O_7$–Fe_2O_3–ThO_2 systems, respectively, are consistent with the changes in the average ionic radius ratio at the A-sites and B-sites. These results suggest that the addition of lanthanides and actinides (e.g., Th, U, or Pu) will affect the structural stability, as well as the radiation response behavior of the pyrochlore structure-type.

PACS: 61.82.−d; 61.80.Jh; 81.40.Wx; 72.80.Ng

1. Introduction

Fluorite and fluorite-related materials, such as isometric pyrochlores, have been proposed as potential host phases for the immobilization of fissile Pu from dismantled nuclear weapons and the 'minor' actinides (e.g., Np, Am, Cm) generated by the nuclear fuel cycle [1–9]. The radiation response of pyrochlore structured compounds, particularly stoichiometric compositions including rare-earth titanates [10–13], zirconates [14,15] and stannates [16,17] have been systematically studied by ion beam irradiations in order to simulate radiation

* Corresponding author. Address: Department of Geological Sciences, University of Michigan, Ann Arbor, MI 48109, USA. Tel.: +1 734 763 9295; fax: +1 734 647 5706.
E-mail address: rodewing@umich.edu (R.C. Ewing).

0022-3115/$ - see front matter © 2007 Elsevier B.V. All rights reserved.
doi:10.1016/j.jnucmat.2007.01.097

damage from the α-decay events of the incorporated actinides. For example, the titanate pyrochlore composition, $Gd_2Ti_2O_7$, the primary host matrix currently being considered, undergoes irradiation-induced amorphization by either α-decay damage [18] or heavy ion beam irradiations at a relatively low dpa (displacements per atom) dose of ~0.18 [11,12]. The factors affecting the radiation response of pyrochlore compounds have been discussed in terms of the bond-type, relative cationic size of A- and B-sites and the deviation from the ideal fluorite structure. Both cation ionic radii and the electronic structure account for the varied responses of pyrochlore structures to ion beam irradiation [12,14–17].

Most of ion beam irradiation experiments were performed on stoichiometric $A_2B_2O_7$ pyrochlore compositions, and very limited data are available for actinide-doped phases. The self-irradiation effects from the α-decay events of incorporated actinides in the transplutonium–zirconate pyrochlores $An_2Zr_2O_7$ (An = Am, Cf) were recently completed [19]. For Zr-based actinide pyrochlores, a phase transformation from a pyrochlore structure to a defect fluorite-type structure was observed with the retention of crystallinity. Unfortunately, the samples doped with α-emitter are limited and the study of self-irradiation is time consuming despite the use of actinides with short half-lives (e.g., ^{249}Cf, ^{244}Cm, ^{238}Pu). By synthesizing materials doped with actinides, the structural transformation in actinide-doped phases upon α-decay damage can be simulated by ion beam irradiations. The critical amorphization dose and amorphization temperature can be determined, which allow the long term performance assessment of waste forms loaded with actinides. In this paper, the yttrium titanate pyrochlores doped with Th and Fe, typical component of some waste stream compositions, were synthesized. Furthermore, $Y_2Ti_2O_7$ pyrochlores doped with La have been sintered with the designed compositions for the $(Y_{1-x}La_x)_2Ti_2O_7$ system ($x = 0$, 0.08, 0.5, and 1). Lanthanum and other light lanthanides (from Ce to Gd) are a major component of the REE/actinide fraction separated from HLW. The effects of the incorporation of lanthanum and Th on the structural stability and radiation response of the yttrium titanate pyrochlores were investigated by X-ray diffraction and ion beam irradiation, respectively.

2. Experimental

2.1. Sample synthesis and characterization

Powdered samples with the designed compositions of $(La_xY_{1-x})_2Ti_2O_7$ ($x = 0$, 0.08, 0.5, and 1) were prepared by solid-state reaction of TiO_2 with Y_2O_3 and La_2O_3 powders in air at 1373 K for 12 h. The Th-doped samples were synthesized by sintering $Y_2Ti_2O_7$ with equal amount (in moles) of Fe_2O_3 and ThO_2 at 1373 K for 12 h. The amount of ($Fe_2O_3 + ThO_2$) varied from 5, 10 and 15 wt%. X-ray diffraction (XRD) was used to monitor the synthesis process and to confirm the formation of the pyrochlore structure. X-ray powder diffraction data were collected using a Scintag PAD-V diffractometer with a Cu anode and an accelerating voltage of 45 kV over an angular range, $2\theta = 10$–$85°$ and a 0.02° step size with a scanning rate of $6.0° \text{ min}^{-1}$. The unit cell of Th- and La-doped $Y_2Ti_2O_7$ were determined by Rietveld refinement based on powder X-ray diffraction data. The pyrochlore structures of synthetic yttrium titanate powdered samples were further confirmed by transmission electron microscopy using a JEOL 2010 F transmission electron microscope (TEM) with a field emission source operated at 200 kV. High resolution TEM images were used to assess the crystallinity of the powdered samples. The TEM samples were prepared by dispersing powdered samples on holey-carbon Cu grids. All powdered samples were stable under 200 keV electron beam irradiation.

2.2. Ion beam irradiation

The response of La and Th-doped $Y_2Ti_2O_7$ to ion beam damage was investigated using 1 MeV Kr^{2+} ion irradiation. Ion irradiation and *in situ* TEM observations were performed using the IVEM-Tandem Facility at the Argonne National Laboratory over the temperature range from 293 to 1173 K. During irradiation, the ion beam was aligned approximately normal to the sample surface. The ion flux is set to be $6.25 \times 10^{11} \text{ cm}^{-2} \text{ s}^{-1}$. To avoid concurrent electron beam irradiation damage, the electron beam was turned off during the ion irradiation. The crystalline-to-amorphous transformation was determined by intermittent observation of the selected-area electron diffraction (SAED) pattern with increasing fluence. The critical amorphization ion fluence (F_c), the fluence at which complete

amorphization occurs, was defined as the fluence at which all of the diffraction maxima in the SAED patterns had disappeared. A number of different grains with pyrochlore structures as evidenced by the SAED patterns were monitored during ion irradiations, and final doses were obtained by averaging the experimental data of those grains. The critical amorphization ion fluence, F_c (cm^{-2}), was converted to the critical dpa dose for amorphization, D_c, using SRIM-2000 calculations [20] assuming a displacement energy of ~50 eV for all atoms in $Y_2Ti_2O_7$ pyrochlores. This value is consistent with the experimental data of $La_2Zr_2O_7$ and $Y_2Ti_2O_7$ determined by time-resolved cathodoluminescence spectroscopy measurements [21].

3. Results and discussion

3.1. $Y_2Ti_2O_7$–$La_2Ti_2O_7$ systems

Pyrochlore superstructures were mainly obtained for the $(La_xY_{1-x})_2Ti_2O_7$ system based on the X-ray diffraction results. A single phase pyrochlore structure was identified for $Y_2Ti_2O_7$. A layered perovskite structure was obtained for the end member of $La_2Ti_2O_7$, as evidenced by the XRD diffraction and TEM observations, in which the distorted TiO_6 octahedra sharing vertices form infinite perovskite-like layers and La atoms occupy distorted perovskite A-site and interlayer sites [22]. Limited amounts of La were incorporated into yttrium titanate pyrochlore structure, as evidenced by energy dispersive X-ray measurements under TEM observation; however, a second phase of $La_2Ti_2O_7$ formed for La-doped compositions. These results are consistent with the phase stability of the formation of pyrochlore structure. For the ordered pyrochlore, $A_2B_2O_7$, the phase stability of the superstructure is basically determined by the A- and B-site cation radius ratio. This cation ionic radius ratio for the stable phase of the ordered pyrochlore has been determined to be between 1.46 ($Gd_2Zr_2O_7$) and 1.78 ($Sm_2Ti_2O_7$). Above the upper radius ratio, the cubic pyrochlore cannot form. With the substitution of larger size La^{3+} ions (1.16 Å) for Y^{3+} (1.019 Å) in the $Y_2Ti_2O_7$ structure [23], the average cation ionic radius ratio r_{A3+}/r_{B4+} increases from 1.68 ($x = 0$) to 1.80 ($x = 0.5$) in the $(La_xY_{1-x})_2Ti_2O_7$ system, which is above the boundary of phase stability of pyrochlore superstructure [24]. Therefore, the pyrochlore structure cannot form with the starting composition of $YLaTi_2O_7$.

The lattice parameters of La-doped yttrium titanate pyrochlores were derived from Rietveld refinements based on the X-ray powder diffraction data. An increase in the lattice parameter of La-doped pyrochlores was found for the samples with higher amounts of La in the starting materials, suggesting that more La was incorporated into the pyrochlore structure. For rare-earth titanate pyrochlores, an approximately linear relationship in the lattice parameter was established as a function of A-site cation ionic radius [24]. The solid-state chemistry of the lanthanides in combination with oxygen is primarily dependent on the ionic size and electronic configuration. In the lanthanides, as electrons are added to the 4f orbital with the increasing atomic number from La to Lu, the electrons in the 4f orbital are effectively shielded by the outer shell of $5d^1$ and $6s^2$ valence electrons, which leads to the stable trivalent state for lanthanide ions [25]. Due to the predominance of ionic bonding between the lanthanide elements and oxygen, the cubic lattice parameter for titanate pyrochlores $A_2Ti_2O_7$ (A = Lu ~ Sm, and Y) displays a nearly linear relation to the ionic radii [24]. Fig. 1 summarizes the cubic lattice parameters of titanate pyrochlores as a function of the average ionic radii of A-site cations. Based on the linear relationship generated from the rare-earth titanate pyrochlores, the average ionic radii at the A-site can be derived for La-doped $Y_2Ti_2O_7$. Therefore, the amount of La, x, incorporated into the pyrochlore structure can be approximately

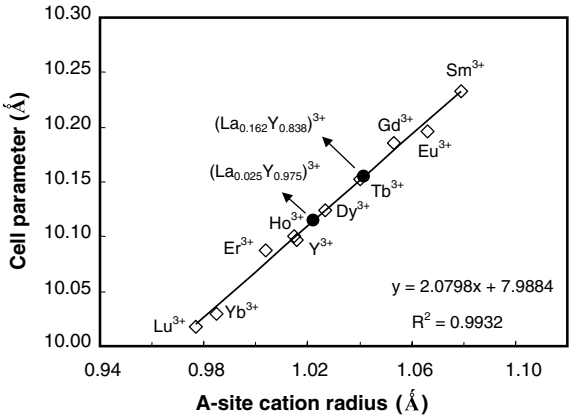

Fig. 1. The cubic lattice parameters of rare-earth titanate pyrochlores [24] and La-doped yttrium titanate pyrochlores as a function of average ionic radii at the A-site.

determined to be 0.025 and 0.162 for the samples with the starting nominal compositions of $(La_{0.08}Y_{0.92})_2Ti_2O_7$ and $YLaTi_2O_7$, respectively.

All of La-doped yttrium titanates were readily amorphized by a 1 MeV Kr^{2+} ion irradiation at room temperature. The characteristic microstructural evolution due to increasing levels of radiation damage (i.e. the gradually decreasing intensity of the diffraction maxima, and the appearance of a diffuse diffraction halo with increasing ion dose) was observed by *in situ* TEM observations. Above the critical amorphization ion fluence, F_c, diffraction maxima from the crystalline domains disappear completely, and the final fully amorphous state was achieved as revealed by SAED patterns. The critical amorphization dose of materials subjected to 1 MeV Kr^{2+} irradiation at room temperature decreases significantly with increasing amount of La (Fig. 2(a)). The temperature dependence of the critical amorphization dose for the titanate pyrochlores irradiated by 1 MeV Kr^{2+} ions is shown in Fig. 2(b). For all of the La-doped yttrium titanates, the critical amorphization dose increases with increasing temperature due to dynamic annealing effects. Above a critical amorphization temperature, T_c, the critical amorphization dose increases to infinity, and complete amorphization does not occur. The critical amorphization temperatures derived from a cascade quench model [26] are 780, 890 and 920 K for $Y_2Ti_2O_7$, $(La_{0.162}Y_{0.838})2Ti_2O_7$ and $La_2Ti_2O_7$, respectively. Based on the critical amorphization dose at room temperature and the critical amorphization temperatures, the susceptibility of materials to ion beam-induced amorphization in $(La_xY_{1-x})_2Ti_2O_7$ system increases with greater amount of La in the structure, and this trend can be extended to the pure end member of $La_2Ti_2O_7$ despite of the change to a layered perovskite structure.

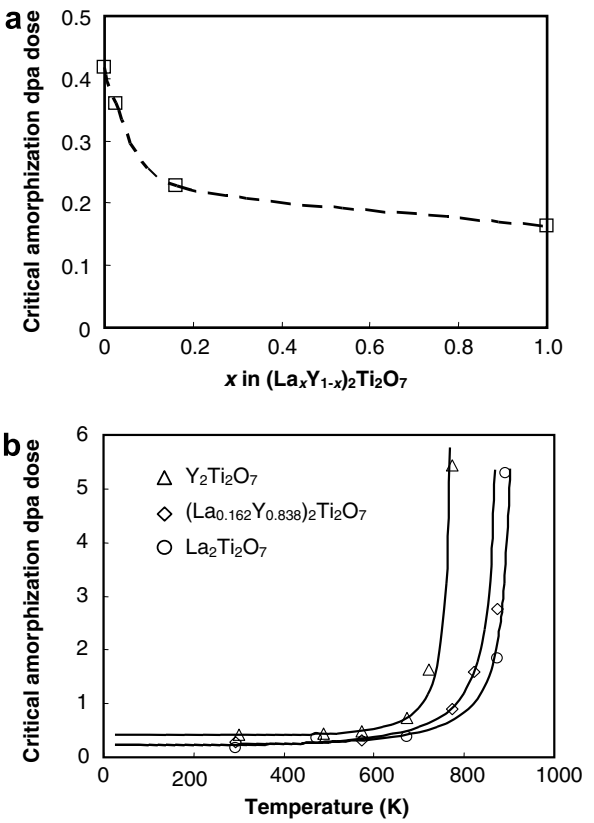

Fig. 2. Critical amorphization dose at room temperature (a) and temperature dependence (b) of the $(La_xY_{1-x})_2Ti_2O_7$ system ($x = 0$, 0.162, and 1) upon 1 MeV Kr^{2+} ion irradiation.

The lower amorphization dose and higher critical amorphization temperature with increasing La-contents in the solid solution of $(La_xY_{1-x})_2Ti_2O_7$ clearly demonstrates the important effects of the incorporation of lanthanide elements on the response behaviour of the pyrochlore structure to radiation-induced amorphization. These results are consistent with recent systematic ion beam irradiation studies on a series of titanate pyrochlores $A_2Ti_2O_7$ (A = Lu to Sm, and Y) [12] and zirconate pyrochlores $A_2Zr_2O_7$ (A = Gd, Eu, Sm and La) [14]. Generally, the 'radiation resistance' of pyrochlores is closely related to the cation ionic radius ratio and x parameter for 48f oxygen. With the decreasing cation ionic radius ratio and increasing x parameter, the pyrochlore structure-type becomes more 'radiation resistant'. The increasing susceptibility of La-doped yttrium titanates to ion beam-induced amorphization can be attributed to the greater average ionic radius of the cations at the A-site as the larger size of La^{3+} is incorporated into the pyrochlore structures.

3.2. Th-doped $Y_2Ti_2O_7$

X-ray diffraction analysis confirmed that pyrochlore structures mainly formed in the Th and Fe-doped samples by sintering $Y_2Ti_2O_7$ and ($ThO_2 + Fe_2O_3$) in air at 1373 K for 12 h. Unlike the stoichiometric $Y_2Ti_2O_7$, in which the pure pyrochlore superstructure was obtained and no detectable impurities were found, residual ThO_2 was identified for Th and Fe-doped samples (Fig. 3). With increasing amounts of $ThO_2 + Fe_2O_3$ in the starting

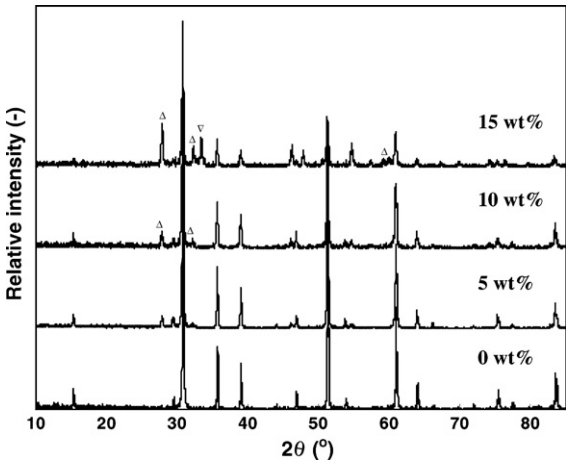

Fig. 3. X-ray diffraction patterns of yttrium titanate pyrochlores doped with various amount of ($Fe_2O_3 + ThO_2$). Pyrochlore structures were mainly observed. The diffraction maxima from residual phases of ThO_2 (labeled by △) and Fe_2O_3 (labeled by ▽) were identified in the X-ray diffraction patterns.

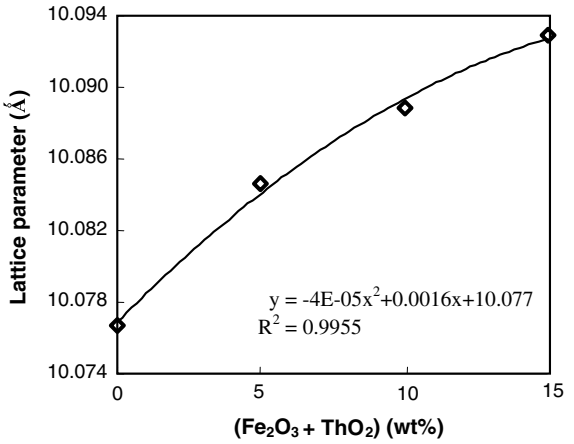

Fig. 4. The cell parameters of pyrochlore structures as a function of amount of ($Fe_2O_3 + ThO_2$) in the starting materials.

materials, the intensity of diffraction maxima from impurities of ThO_2 and Fe_2O_3 increased correspondingly, suggesting that the reaction is not complete under these conditions. Further increasing in the annealing time and sintering temperature may lead to the formation of single phase pyrochlore such that all of the Th and Fe may be incorporated into the $Y_2Ti_2O_7$ crystal structure. As compared with the pure single phase $Y_2Ti_2O_7$, the diffraction peaks of pyrochlore structures shifted slightly to the lower angles of two theta, reflecting the change in the cell parameter upon the incorporation of Th and Fe. Rietveld refinement based on powder X-ray diffraction data indicated that the cell parameter increased as more Th and Fe were incorporated into the pyrochlore structure with greater amounts of ($ThO_2 + Fe_2O_3$) in the starting materials (Fig. 4). Because of the existence of residual ThO_2 and Fe_2O_3 phases in the synthetic powdered samples, a linear relationship between the cell parameter of the pyrochlore structure and doping amounts in the starting materials is not expected. Nevertheless, the variation in the cell parameter can be attributed to the average ionic size difference upon the incorporation of Th^{4+} and Fe^{3+} at the cationic sites of the pyrochlore structure. In the pyrochlore structure, Y^{3+} is 8-coordinated and located in a distorted cube; while, Ti^{4+} is six-coordinated and located in a distorted octahedron. The effective ionic radii of 8-coordinated Th^{4+} and Y^{3+} are 1.05 and 1.019 Å, respectively. The effective ionic radii of Th^{4+} and Ti^{4+} for 6-fold coordination are 0.94 and 0.605 Å, respectively. On the other hand, the incorporation of Fe^{3+} substituting for Y^{3+} may reduce the lattice parameter because the effective ionic radius of Fe^{3+} in the 8-coordination (0.78 Å) is less than that of Y^{3+} (1.019 Å). Therefore, the substitution of Th^{4+} for either Y^{3+} or Ti^{4+} in the yttrium titanate pyrochlore structure appears to be the reason for the increase in the cell parameter. The microstructure and morphology of the Th and Fe-doped powdered samples were further studied by transmission electron microscopy. Fig. 5(a) shows a bright-field TEM image of the synthetic sample doped with 10 wt% ($ThO_2 + Fe_2O_3$). A high resolution TEM image (Fig. 5(b)) confirms the formation of pyrochlore superstructure. EDS spectrum (Fig. 5(c)) acquired from the individual grains with the nm size of electron probe clearly indicated the incorporation of Th and Fe in the crystal structure, consistent with the X-ray diffraction results.

Similar to the yttrium and other rare-earth titanate pyrochlores [11,12], the Th-doped compositions are readily amorphized by 1 MeV Kr^{2+} irradiations at room temperature. Interestingly, a significant increase in the critical amorphization fluence was observed with the increasing amount of ThO_2 and Fe_2O_3 to 15 wt% in the starting material (Fig. 6). The increase in the critical amorphization fluences for the Th-doped samples is consistent with the increase in the cell parameter. As the larger Th^{4+} may substitute for Ti^{4+} at the B-site in the pyrochlore structure, the average cationic ionic radius ratio, r_{A3+}/r_{B4+}, decreases correspondingly such that the pyrochlore structure approaches the

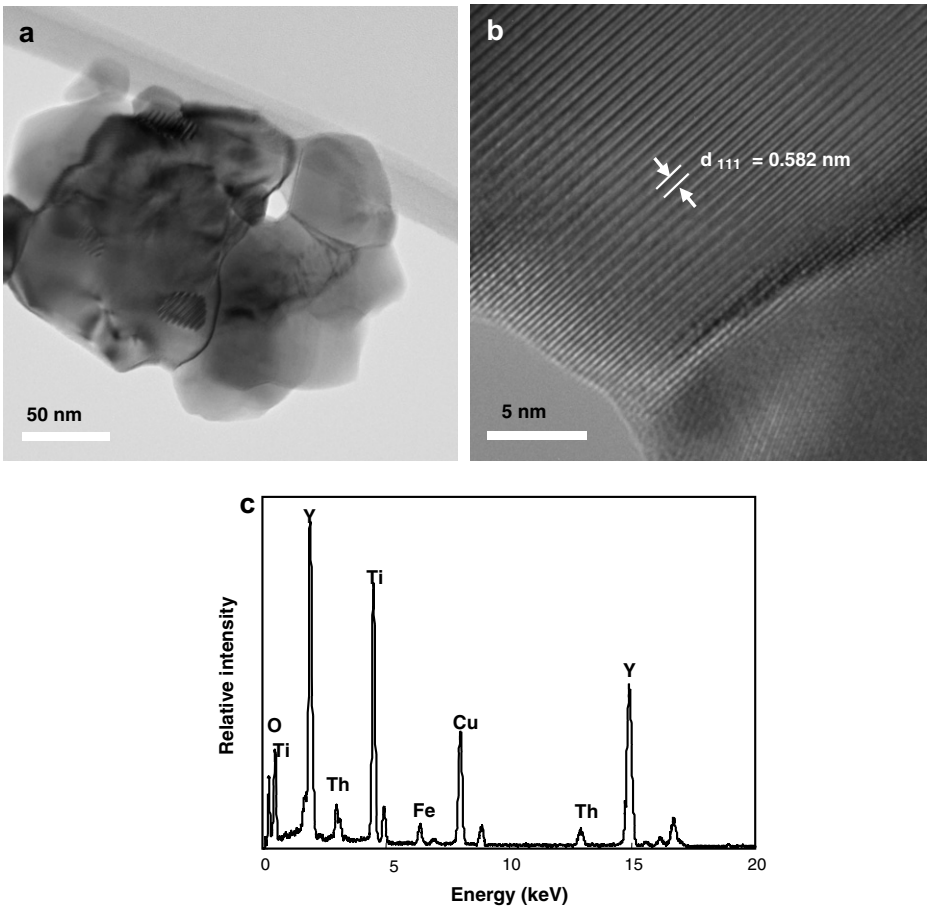

Fig. 5. Bright-field (a) and high resolution (b) TEM images and the EDX spectrum (c) acquired from individual grains of thorium-doped yttrium titanate pyrochlore powdered samples with 10 wt% ($Fe_2O_3 + ThO_2$) in the starting material.

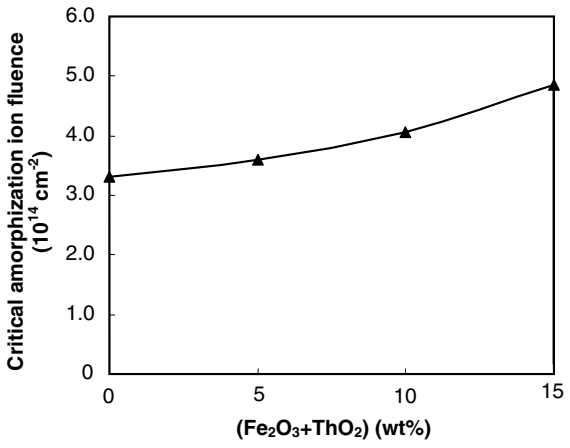

Fig. 6. Critical amorphization fluences of Th-doped yttrium titanate pyrochlores as a function of the concentration of the dopants in the starting materials.

ideal fluorite structure; thus, the structure is more radiation 'resistant', that is it disorders to a defect fluorite structure. This result indicates that the addition of Th may further enhances the 'radiation resistance' of pyrochlores used as waste forms for the immobilization of actinides.

4. Conclusions

Lanthanum- and thorium-doped yttrium titanate pyrochlores have been synthesized by solid-state reaction at 1373 K in air for 12 h, and their radiation response were investigated by 1 MeV Kr^{2+} ion irradiation under *in situ* TEM observation. Single phase pyrochlore structures did not form in the La-doped compositions; while the end member of $La_2Ti_2O_7$ formed a layered perovskite structure. Residual ThO_2 and Fe_2O_3 were identified for Th and Fe-doped powdered samples. All of La and Th-doped powdered samples are readily amorphized at room temperature. A greater susceptibility to ion beam-induced amorphization was found with

increasing La contents for the $(La_xY_{1-x})_2Ti_2O_7$ binary system, as evidenced by the lower critical amorphization dose and higher critical amorphization temperature. In contrast, the critical amorphization fluences increase significantly for Th-doped yttrium titanate pyrochlores as the amount of (ThO_2 + Fe_2O_3) in the starting materials increased. The variation in the phase stability and radiation response behaviour of lanthanum and thorium-doped yttrium titanate pyrochlores can be explained by the average cationic radius ratio criteria. These results indicate that the incorporation of rare-earth elements and actinides into the pyrochlore structure affect both the structural stability and the materials' radiation response behaviour.

Acknowledgements

We are grateful to the staff of the IVEM-Tandem Facility at the Argonne National Laboratory for assistance during ion irradiation experiments. This work was supported by the Office of Basic Energy Sciences, US Department of Energy under DOE Grants DE-FG02-97ER45656.

References

[1] R.C. Ewing, W.J. Weber, J. Lian, J. Appl. Phys. 95 (2004) 5949.
[2] K.E. Sickafus, L. Minervini, R.W. Grimes, J.A. Valdez, M. Ishimaru, F. Li, K.J. McClellan, T. Hartmann, Science 289 (2000) 748.
[3] W.J. Weber, R.C. Ewing, Science 289 (2000) 2051.
[4] W.J. Weber, R.C. Ewing, Mater. Res. Soc. Symp. Proc. 713 (2002) 443.
[5] B.D. Begg, N.J. Hess, W.J. Weber, R. Devanathan, J.P. Icenhower, S. Thevuthasan, B.P. McGrail, J. Nucl. Mater. 288 (2001) 208.
[6] K.B. Helean, A. Navrotsky, E.R. Vance, M.L. Carter, B. Ebbinghaus, O. Krikorian, J. Lian, L.M. Wang, J.G. Catalano, J. Nucl. Mater. 303 (2002) 226.
[7] J. Lian, L.M. Wang, S.X. Wang, J. Chen, L.A. Boatner, R.C. Ewing, Phys. Rev. Lett. 87 (2001) 145901.
[8] A.A. Digeos, J.A. Valdez, K.E. Sickafus, S. Atio, R.W. Grimes, A.R. Boccaccini, J. Mater. Sci. 38 (2003) 1597.
[9] S.S. Shoup, C.E. Bamberger, R.G. Haire, J. Am. Ceram. Soc. 79 (1996) 1489.
[10] S.X. Wang, B.D. Begg, L.M. Wang, R.C. Ewing, W.J. Weber, K.V.G. Kutty, J. Mater. Res. 14 (1999) 4470.
[11] S.X. Wang, L.M. Wang, R.C. Ewing, G.S. Was, G.R. Lumpkin, Nucl. Instrum. and Meth. B 148 (1999) 704.
[12] J. Lian, J. Chen, L.M. Wang, R.C. Ewing, J.M. Farmer, L.A. Boatner, K.B. Helean, Phys. Rev. B 68 (2003) 134107.
[13] J. Lian, L.M. Wang, R.C. Ewing, L.A. Boatner, Nucl. Instrum. and Meth. B 241 (2005) 365.
[14] J. Lian, X.T. Zu, K.V.G. Kutty, J. Chen, L.M. Wang, R.C. Ewing, Phys. Rev. B 66 (2002) 054108.
[15] J. Lian, L.M. Wang, R.G. Haire, K.B. Helean, R.C. Ewing, Nucl. Instrum. and Meth. B 218 (2004) 236.
[16] J. Lian, R.C. Ewing, L.M. Wang, K.B. Helean, J. Mater. Res. 19 (2004) 1575.
[17] J. Lian, K.B. Helean, B.J. Kennedy, L.M. Wang, A. Navrotsky, R.C. Ewing, J. Phys. Chem. B 110 (2006) 2343.
[18] W.J. Weber, F.P. Roberts, Nucl. Technol. 60 (1983) 178.
[19] R.E. Sykora, P.E. Raison, R.G. Haire, J. Solid State Chem. 178 (2005) 578.
[20] J.F. Ziegler, J.P. Biersack, U. Littmark, The Stopping and Range of Ions in Solids, Pergamon, New York, 1985.
[21] K.L. Smith, M. Collela, R. Cooper, E.R. Vance, J. Nucl. Mater. 321 (2003) 19.
[22] H.W. Schmalle, T. Williams, A. Reller, A. Linden, J.G. Bednorz, Acta Crystallogr. B 49 (1993) 235.
[23] R.D. Shannon, Acta Crystallogr. A 32 (1976) 751.
[24] M.A. Subramanian, G. Aravamudan, G.V.S. Rao, Prog. Solid State Chem. 15 (1983) 55.
[25] L.R. Morss, Handbook on the Physics and Chemistry of Rare Earths, vol. 18, North-Holland, Amsterdam, 1994.
[26] S.X. Wang, L.M. Wang, R.C. Ewing, Phys. Rev. B 63 (2001) 024105.